Eelgrass and Macroalgal Mapping to Develop Nutrient Criteria in New Hampshire's Estuaries using Hyperspectral Imagery

Authors: Pe'eri, Shachak, Morrison, J. Ru, Short, Fred, Mathieson, Arthur, and Lippmann, Thomas

Source: Journal of Coastal Research, 76(sp1) : 209-218

Published By: Coastal Education and Research Foundation

URL: https://doi.org/10.2112/SI76-018

Journal of Coastal Research	SI	76	209–218	Coconut Creek, Florida	2016

Eelgrass and Macroalgal Mapping to Develop Nutrient Criteria in New Hampshire's Estuaries using Hyperspectral Imagery

Shachak Pe'eri[†*], J. Ru Morrison[‡], Fred Short[§], Arthur Mathieson[§] , and Thomas Lippmann[†]

[†]Center for Coastal and Ocean Mapping
University of New Hampshire
Durham, NH 03824, U.S.A.

[‡]National Oceanic and Atmospheric Administration/National Ocean Service
NERACOOS
Rye, NH 03870, U.S.A.

[§]Jackson Estuarine Laboratory
University of New Hampshire
Durham, NH 03824, U.S.A.

www.cerf-jcr.org

www.JCRonline.org

ABSTRACT

Pe'eri, S.; Morrison, J.R.; Short, F.; Mathieson, A., and Lippmann, T., 2016. Eelgrass and macroalgal mapping to develop nutrient criteria in New Hampshire's estuaries using hyperspectral imagery. *In*: Brock, J.C.; Gesch, D.B.; Parrish, C.E.; Rogers, J.N., and Wright, C.W. (eds.), *Advances in Topobathymetric Mapping, Models, and Applications*. *Journal of Coastal Research*, Special Issue, No. 76, pp. 209–218. Coconut Creek (Florida), ISSN 0749-0208.

In recent years, mapping of seagrass beds for assessment of water quality has become more common in the United States and around the world. The static location of seagrass on marine sediments and its sensitivity to light make it a good environmental indicator and an alternative to water sampling of suspended particulates and dissolved matter. The New Hampshire (NH) Department of Environmental Services (DES) adopted the assumption that eelgrass survival could be used as the water quality target for nutrient criteria in NH's estuaries. One of the hypotheses put forward regarding eelgrass decline in the Great Bay Estuary (GBE) is that a eutrophication response to nutrient increases caused proliferation of nuisance macroalgae. This paper presents an eelgrass and macroalgae mapping procedure using hyperspectral imagery (HSI) collected by an AISA Eagle sensor. In addition to HSI, an external source bathymetric dataset provided a key dataset in the procedure. The bathymetric dataset was used to correct for light attenuation by the water column for resolving bottom reflectance and to calculate the extinction depth of light in the estuary's water for mapping areas that are optically deep. The procedure was developed in the Environment for Visualizing Images (ENVI) and includes two separate approaches based on the available spectral ranges for mapping vegetation above and below the water. A composite eelgrass and macroalgal map was produced over Great Bay proper. A high level of correlation was found between the eelgrass results to more detailed eelgrass maps (above 30% density) produced from aerial imagery and ground truthing. Little quantitative verification for the macroalgal data was available beyond a visual inspection. The two datasets showed good correlation. Based on the procedural results and long-term eelgrass mapping data, numeric nutrient criteria for NH's estuaries were developed.

ADDITIONAL INDEX WORDS: *Great Bay Estuary, eelgrass, macroalgae, bathymetric dataset, hyperspectral imagery, light attenuation*.

INTRODUCTION

One of the main indicators used for water quality evaluation is the amount of suspended particulates and dissolved matter in the water column, which includes phytoplankton, Colored Dissolved Organic Matter (CDOM), and non-algal particles (Bricker *et al*., 2008). The ability to collect water samples over a large area in a short amount of time with sufficient spatial distribution is limited, mainly because marine waters are a dynamic medium that is constantly changing (on the order of minutes to hours). An alternative approach for assessing water quality is mapping the spatial distribution of submersed aquatic vegetation (SAV). The logistical motivation for this approach is that SAV is a more stable indicator (rate of change is on the order of days to weeks) than suspended particulates or dissolved matter. However, water attenuation can pose a challenge to identify bottom reflectance as SAV and requires ground truthing to support the classification results.

DOI: 10.2112/SI76-018 received 16 December 2014; accepted in revision 31 July 2015.
*Corresponding author: Shachak@ccom.unh.edu

The New Hampshire (NH) Department of Environmental Services (DES) has investigated new water quality standards to replace the previous narrative standards that were difficult to apply in impairment and permitting decisions (Trowbridge, 2009). A numerical standard provides a clear definition and guides future policy decisions for the protection of the water resources. Eelgrass, *Zostera marina*, is a common benthic indicator used to evaluate water quality (Beem and Short, 2009; Short, 2012; Short and Burdick, 1996). The NH DES hypothesis was that losses of eelgrass are directly related to reduction in light conditions or proliferation of macroalgae (Costa *et al.*, 1992; Short, Burdick, and Kaldy, 1995). In 2005, NH DES initiated a study of the Great Bay Estuary (GBE) based on preliminary results that showed nitrogen concentrations had increased by 59% in the previous 25 years and historic eelgrass beds had lost 29% coverage over the previous 60 years (Trowbridge, 2009). The nitrogen loading rates measured in Great Bay were higher (182 kg/ha/yr) than other eutrophic estuaries in the Gulf of Maine, such as Waquoit Bay, MA (>60 kg/ha/yr; Hauxwell, Cabrien, and Valiela, 2003; Valiela *et al.*, 1992, 1997). In addition, a concern arose for the eelgrass habitat in Great Bay due to the proliferation of green and red nuisance

macroalgae, such as *Ulva* and *Gracilaria* (Trowbridge, 2009). Such macroalgae can eliminate eelgrass habitat when they form dense mats (Short and Burdick, 1996).

Previous work to map eelgrass beds in GBE was conducted manually using RGB aerial imagery and field surveys (Macleod, Congalton, and Short, 1995; Short, 2012). Aerial and satellite imagery with high resolution on the order of 0.1 to 2.0 m per pixel can allow the operator to resolve vegetation patches in shallow waters (Moore and Wetzel, 2000); however, the broad spectral band (~150 nm) cannot easily resolve eelgrass from wetland vegetation or green macroalgae (Dekker *et al.*, 1996; McKenzie, Finkbeiner, and Kirkman, 2001). This paper presents HSI as an alternative quantitative approach to RGB aerial imagery. Light attenuation in the water column was corrected using a bathymetric dataset. The procedure was developed for the NH DES using an ENVI environment to map eelgrass and macroalgal beds. In addition, the bathymetric dataset was used to calculate the extinction depth for areas that are optically deep. The HSI for the study was collected on August 29, 2007, using an AISA Eagle sensor over the GBE, NH/Maine. A comprehensive eelgrass and macroalgae map of the estuary was produced and verified with ground truth, and the results were compared to detailed eelgrass maps produced from aerial imagery and ground truth (Short, 2012). The results of the study were used to support NH DES in the development of a water clarity standard for nutrient criteria in the GBE.

METHODS

Radiative Transfer Models and Spectral Characteristics

In recent years, there has been an increase in studies investigating optical remote sensing for mapping seagrass and macroalgae. Healthy vegetation typically contains chlorophyll-*a*, a pigment that generates a spectral response characterized by a steep slope at around 680–690 nm (*i.e.*, the red edge) in between a strong red wavelength absorption and a near-infrared reflection (Kirk, 1994). However, in the marine environment, this red-edge spectral response can only be clearly observed above water or in shallow areas, 1 or 2 m, depending on water clarity because of scattering and absorption by phytoplankton, suspended matter, and dissolved organic matter (DOM) that restrict the passage of light underwater (Dekker *et al.*, 2002). Bottom reflectance from SAV is typically low and often lower than reflectance over optically deep waters. In addition, self-shading within the canopy further reduces the amount of returning energy (Zimmerman, 2003).

Various macroalgal species grow under a low amount of light that ranges from 0.1% to 1% of the surface irradiance. However, seagrass vegetation requires much higher light levels that range from 10% to 37% of the surface irradiance (Duarte, 1991; Ochieng, Short, and Walker, 2010; Olesen and Sand-Jensen, 1993; Zimmerman, 2006). The light sensitivity of seagrass beds makes them a very useful environmental indicator for deteriorated water quality (Short and Wyllie-Echeverria, 1996) and can be mapped by optical remote sensing in more favorable conditions. Previous studies have shown that the leaf reflectance of seagrass characteristics can exhibit a broad peak (530 nm to 570 nm) centered at 550 nm, a trough at 670–680 nm, and a sharp transition (increase) to 700 nm (the red edge) with a gently decreasing infrared plateau above 750 nm (Alberotanza, Cavalli, and Zandonella, 2006; Dekker *et al*., 2006; Drake, Dobbs, and Zimmermann, 2003; Fyfe, 2003; Karpouzli, Malthus, and Place, 2004; Thorhaug, Richardson, and Berlyn, 2007). Macroalgal species, on the other hand, vary in spectral characteristics based on their pigments. For example, two common north-Atlantic algal species, *Fucus vesiculosus* (brown alga), and *Ulva lactuca* (green alga) are spectrally different in the 530 nm to 580 nm range and at 680 nm (Karpouzli, Malthus, and Place, 2004; Thorhaug, Richardson, and Berlyn, 2007; Wezermak, Turner, and Lyzenga, 1976). Furthermore, the spectral characteristics of seagrass and green algae are similar in the 400–530 nm and 580–680 nm ranges, as chlorophyll-*a* is the predominant pigment in both seagrass and green seaweeds (Thorhaug, Richardson, and Berlyn, 2007).

Water column mapping using hyperspectral data is an emerging field. Hyperspectral data collected from remote sensing platforms (*e.g.*, airborne or satellite) or *in situ* (*e.g.*, buoys) can potentially detect optical water quality concentrations, such as colored dissolved organic matter, chlorophyll, and suspended matter (Brando and Dekker, 2003; Kirkpatrick *et al.*, 2003; Yu *et al.*, 2010). Water quality can also affect the mapping results. As a first-order approximation, the water column is considered uniform above the mudflats, where eelgrass beds may be present. Although observations of water quality were conducted during this study (Morrison *et al.*, 2008; Trowbridge, 2009), the topic is beyond the scope of this study.

In addition to the spectral characteristics of bottom reflectance, R_b, the observed remote sensing reflectance over a seagrass bed is dependent on the water depth, z, diffuse attenuation coefficient, k, and the remote sensing reflectance over optically deep waters, R_w (Beiwirth, Lee, and Burne, 1993; Dekker *et al.*, 2006; Dierssen *et al.*, 2003; Philpot, 1989):

$$R_{rs} = R_w + (R_b - R_w) \cdot e^{-2 \cdot z \cdot k} \qquad (1)$$

The calculation assumes a homogeneous water body and no contribution from the atmosphere. A uniform water-body condition assumption is valid in an inlet environment when investigating only mudflat areas. Thus, inlet's channels that contained stronger currents and more suspended matter were ignored as channel water may have different optical conditions than the water above the mudflats. Also, the diffuse attenuation coefficients for upwelling and downwelling light are assumed to be the same.

More studies have investigated the optical behavior of seagrass than of submerged macroalgae. A large diversity of macroalgal types with different pigments can be found in a given study site that complicate mapping different macroalgal species as a single class or multiple classes (Mathieson and Penniman, 1986, 1991; McGlathery, Sundback, and Anderson, 2007). As outlined by Dring (1991), the main macroalgal species found in coastal and estuarine environments can be characterized by their pigments: greens (*chlorophylls a* and *b, carotenes,* and *xanthophylls*), browns (*chlorophylls a* and *c, and fucoxanthin*), and reds (*chlorophyll a, phycoerythrin, phycocyanin, carotenes, lutein,* and *zeaxanthin*). Vahtmäe *et al.* (2006) investigated the spectral characteristics of green, brown, and red algae in different water clarity conditions and found clear spectral differences over a large spectral range (450 nm to

720 nm). However, these differences are blurred underwater. Similar conclusions were observed by Casal *et al.* (2012), who investigated mapping procedures for exposed green, brown, and red algal beds during low tides using HSI. In addition to direct spectral characteristics, it is also important to understand the spectral resolution and characteristics of the observing sensor.

Classification Procedures

Early studies on seagrass and macroalgae mapping focused on vegetation exposed above low tide (*e.g.*, Mumby *et al.*, 1997). The algorithms used in these methods typically utilized a spectral range between 400 nm to 700 nm and sometimes also included the infrared range (greater than 700 nm). The general structure of all these procedures is typically the same and includes two main steps: 1) extract the area between high water (the shoreline at high tide) and the low shoreline that is apparent in the imagery; and 2) apply a set of classifiers (decision tree) to map the habitat or extract specific features. The common classifiers used for eelgrass/macroalgal mapping procedures include band ratios and indices (Penuelas *et al.*, 1993; Zibordi, Parmiggiani, and Alberotanza, 1990), supervised classification using statistical distance (Larsen *et al.*, 2009; Peneva, Griffith, and Carter, 2008; Phinn *et al.*, 2008), unmixing (Alberotanza, Cavalli, and Zandonella, 2006); Spectral Angle Mapper (Peneva, Griffith, and Carter, 2008); principal component analysis (Ferguson and Korfmacher, 1997; Pasqualini *et al.*, 2005), and ISODATA/CLUSTER classification (Ackelson and Klemas, 1987). These mapping procedures are successful in macro-tidal environments (*i.e.*, a tidal range greater than 4 m) with a time window long enough to acquire imagery of the vegetation at exposed conditions (Larsen *et al.*, 2009). However, within mid-Atlantic and northeastern coastal areas of the United States, it is more common to find seagrass and salt marshes in meso-tidal (1 m to 4 m) environments or even in areas with a smaller tidal range. Thus, it is very hard to coordinate a survey using aerial or satellite imagery at the lowest tides possible, and the available imagery includes both exposed and submerged vegetation. As a result, the classification approaches mentioned above may perform poorly in these survey cases (Ackelson and Klemas, 1987; Mumby *et al.*, 1997; Penuelas *et al.*, 1993). Furthermore, a simplified radiative transfer model approach assumes the bottom as a Lambertian surface, which might not be suitable for vegetation mapping (Philpot *et al.*, 2004). Thus, water column correction using satellite-derived bathymetry (*e.g.*, Lyzenga, Malinas, and Tanis, 2006; Pe'eri *et al.*, 2014) from aerial or satellite imagery may introduce noise that can confuse classifiers and generate errors in habitat mapping (Kutser, Miller, and Jupp, 2006). Turbid waters that are common in many marshes and wetlands pose an even greater challenge for mapping with multispectral/hyperspectral imagery (Vahtmäe *et al.*, 2006).

Study Site

The study was conducted in Great Bay proper, NH, a tidally dominated system (water supply is from the Gulf of Maine) with river discharge that includes terrestrial and anthropogenic suspended matter (Figure 1). Great Bay proper has the biggest eelgrass habitat in Great Bay Estuary (GBE), both in volume and spatial distribution. The average tidal range in Great Bay is 1.85 m, and the water surface covers 23 km^2 at Mean High Water and 11 km^2 at Mean Lower Low Water (NOAA, 2013). Intertidal areas in Great Bay are mostly mudflats with eelgrass, macroalgae, and intertidal salt marsh vegetation (Chock and Mathieson, 1983; Hardwick-Witman and Mathieson, 1983; Josselyn, 1978; Josselyn and Mathieson, 1980; Mathieson and Hehre, 1986; Short, 1992).

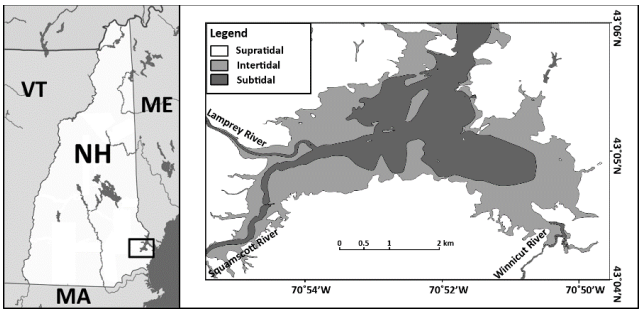

Figure 1. Great Bay study site delineated into dry land (supratidal), intertidal, and subtidal areas. NH – New Hampshire; MA – Massachusetts; ME – Maine; VT – Vermont.

Typically, eelgrass (*Zostera marina*) beds in GBE serve as sediment traps and help to stabilize bottom sediments (Odell *et al.*, 2006). Additionally, eelgrass beds filter estuarine waters, removing both nutrients and suspended sediments from the water column (Jackson, 1944; Short and Short, 1984). However, too many nutrients from wastewater effluent and fertilizers can produce algal blooms that can shade and destroy eelgrass habitats in GBE and elsewhere (Bricker *et al.*, 2008; Short, 1992). In the last few decades, seagrass habitats in GBE have diminished due to both natural and anthropogenic causes (Short and Wyllie-Echeverria, 1996). Most of this decline can be attributed to eutrophication caused by increased nutrient loading associated with the development of coastal zones (Short and Burdick, 1996) or periodic outbreaks of wasting disease from the slime mold *Labryrinthula zosterae* (Jackson, 1944; Milne and Milne, 1951; Short *et al.*, 1986). Studies of macroalgae in the estuary identified multiple species of *Ulva* (*e.g.*, *U. intestinalis* and *U. lactuca*) and *Gracilaria* (*e.g.*, *G. tikvahiae* and *G. vermiculophylla*), epiphytic red algae (*e.g.*, ceramialean red algae) and detached/entangled *Chaetomorpha* populations (Chock and Mathieson, 1983; Hardwick-Witman and Mathieson, 1983). In addition, sedimentation and erosion occur in areas where eelgrass is no longer present to anchor bottom sediments (Beem and Short, 2009; Short *et al*., 1986). The most recent dramatic declines in Great Bay are due to an outbreak of wasting disease in 1989, when the eelgrass area coverage was only 300 acres or 15% of normal levels (Short, 2009). The last maximum extent of eelgrass in the GBE was observed in 1996 after the beds had recovered from a wasting disease episode. Since 1996, Great Bay has lost 45% of its eelgrass distribution and 66% of its eelgrass biomass (Figure 2). The cause of the

most recent decline in eelgrass biomass, observed over the past two decades (1996–2012), is assumed to be related to water quality declines that are linked to nitrogen enrichment and resulting proliferation of macroalgae (Beem and Short, 2009; Short, 2012; Trowbridge, 2009).

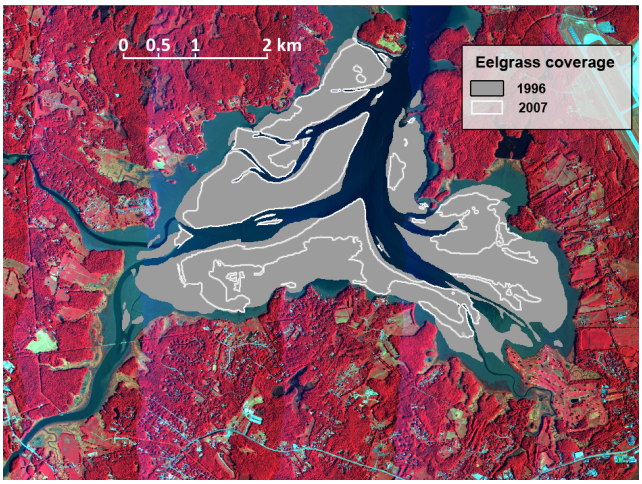

Figure 2. Extent of eelgrass beds in Great Bay in 1996 and 2007 (Short, 2012) overlaid on the hyperspectral false color image mosaic (R: 814 nm, G: 670 nm B: 527 nm channels).

Data

The hyperspectral aerial survey was conducted over GBE using an AISA Eagle sensor. The survey was conducted on August 29, 2007, with the center time for the central line over Great Bay of 08:57 local time (12:57 GMT) and with 8 lines of data collection oriented approximately north-south (30% overlap between two adjacent lines). The acquisition of the hyperspectral imagery was coordinated with the semi-diurnal low tide in Great Bay proper, predicted to be at 08:49 local time during the survey date. The tide-coordinated imagery provided spectral information in the imagery that included both exposed and submerged vegetation. The hyperspectral imagery was collected over 64 spectral channels from approximately 430 nm to 1,000 nm and at a spectral resolution of about 10 nm with a ground resolution of 2.5 m. As a result, part of the study area was submersed and part was exposed. Reference eelgrass coverages were digitized manually using aerial RGB imagery collected in 2007 (Short, 2009). The digitized polygons were segmented based on density and were used as reference to evaluate the performance of the developed procedure (Short, 2009). Manual mapping of eelgrass was conducted according to the NH DES procedures by the University of New Hampshire's (UNH's) Eelgrass monitoring program (Short and Trowbridge, 2003). Eelgrass aerial cover classes were determined using easily identifiable image categories: small detectable patches or sparse plants, 10–30% eelgrass cover; area half covered by eelgrass vs. other bottom (sediment, macroalgae or hard bottom), 30–60%; some other bottom evident in areas of mostly eelgrass, 60–90%; no other bottom evident in the eelgrass area, 90–100%. Digitization of eelgrass cover was conducted by an experienced operator (Fred Short) into ArcMap shapefile polygons according to the identifiable cover class categories. From the manually digitized dataset, it was determined that the extent of eelgrass in Great Bay was considerably smaller (5.04 km^2) in 2007 than the peak coverage observed in 1996 of 9.80 km^2 acres (Figure 2). Although macroalgal mats were noticeable in the 2007 aerial RGB imagery, they were not mapped under UNH's Eelgrass monitoring program. Environmental information on the water conditions over a seven-year period (2000 to 2007) before and during the HSI survey was provided through NOAA's Great Bay National Estuarine Research Reserve System Wide Monitoring Program, the UNH Tidal Water Quality Monitoring Program, and the U.S. Environmental Protection Agency (EPA) National Coastal Assessment program.

During the hyperspectral survey, there was no bathymetric dataset that could be used to correct for water attenuation of light. The available survey soundings were collected by the U.S. Coast and Geodetic Survey (a NOAA predecessor agency) dating from 1913 and 1953–1954, and they could only provide a very coarse bathymetric dataset that most likely is outdated (Jakobsson *et al.*, 2005). Instead, a new bathymetric digital elevation model (DEM) for Great Bay was compiled from surveys conducted over a five-month period (July–November, 2009) using a combination of three survey vessels equipped with single-beam echosounders and differential GPS receivers. Two of these surveys were conducted using flat-bottomed Carolina Skiffs. The echosounders were 50/200 khz dual frequency, one a Knudson 320BP and the other an Odom CV-200, with each being sampled at 20 hz. The third survey was conducted using a Coastal Bathymetry Survey System (CBASS), consisting of a dual-transducer 192 khz single beam echosounder (Lippmann and Smith, 2009). Inter-comparisons between filtered survey data from all three systems showed a mean offset of less than 3 cm, and with 28 cm RMS differences for all overlapping data within a 0.5-m horizontal radius when the time between data points was less than one day. Erroneous bottom detects (noise) due to backscatter from mid-water detritus, fishing gear, or biology were temporally filtered by computing histograms of the data over approximately 2.5-second intervals and setting difference thresholds based on the median value (Lippmann and Smith, 2009). Depth measurements of the vegetation canopy were kept and compiled into a 2.5-m DEM grid. The vertical datum of the DEM was shifted from an ellipsoidal WGS-84 to the apparent shoreline marker (*i.e.*, land/water interface at the time of the survey). In addition, underwater video imagery and *in situ* spectral measurements were collected in 2009 as ground truth measurements to evaluate the hyperspectral imagery. Because of the time period that passed between the hyperspectral aerial survey and ground truth spectral measurement (*i.e.*, two years), the *in situ* measurements were used as a qualitative reference to the spectral characteristics of the different classes (bottom and vegetation) in the study area. The training set for the classification procedure was generated from the hyperspectral imagery.

Discrimination Procedure

Pre-processing

A radiometric correction was applied to the imagery over submersed areas in order to compensate for water attenuation. First, the submersed areas of Great Bay were separated from the exposed land areas using the near-infrared (NIR) channel. Water is essentially opaque in the infrared, making water appear much darker relative to land in the imagery. From the available infrared bands, the 863-nm channel was selected because its imagery showed the most contrast between land and water. The separation between the two areas marked the apparent shoreline boundary (land/water interface) at the time of the survey and serves as the zero-depth marker.

The water clarity and extinction depth of GBE waters at the time of the survey were calculated using the reference DEM. Reflectance of the bottom sediment, R_b, was assumed to be identical to the reflectance of exposed, saturated mud. From the aerial hyperspectral dataset, a reference spectrum for the exposed bottom was produced from 65 pixels over intertidal areas in Great Bay outside the submersed areas. A deep-water spectrum representing the water reflectance, R_w, was produced using an average value of 200 pixels over areas that were deeper than the extinction depth. In addition, 125 spectra were sampled along submersed areas from optically deep areas up to the shoreline in order to calculate the diffuse attenuation coefficient, k, and the extinction depth. The radiometric correction to the imagery was applied using Equation 1:

$$R_b == \frac{R_{rs} - R_w}{e^{-2 \cdot z \cdot k}} + R_w \qquad (1)$$

The diffuse attenuation curve was calculated using a linear fit on the normalized depth spectrum values as a function of water depth. The water clarity was classified as Case 3 Jerlov coastal waters (Jerlov, 1976), associating a diffuse attenuation coefficient for each channel. In addition, the extinction depth that marks the lower depth boundary was measured to be 0.9–1.1 m according to the procedure described by Pe'eri *et al.* (2014). Spectral measurements at depths greater than the extinction depth were masked because the observed reflectance of these submersed areas represents light returning only from the water column and can be considered as noise that can reduce the performance of the mapping procedure.

In addition to the exposed bottom and optically-deep waters, three additional spectral signatures of specific vegetation types in Great Bay proper were generated using Regions of Interest (ROI) taken from above-water sites containing the same underwater bottom features (Figure 3). As described in Equation 1, optically-deep waters are considered to be areas with reflectance from only the water-column scattering with no contribution from the bottom. The statistical analysis of these spectral signatures includes the average value, range (minimum-maximum), and the standard deviation of the reflectance values as a function of wavelength. The three main spectral signatures of vegetation used in the classification process included eelgrass, macroalgae, and wetland vegetation (*i.e.*, *Spartina alterniflora*). A green return is observed in the spectral signature of the optically-deep water class. The return may be related to

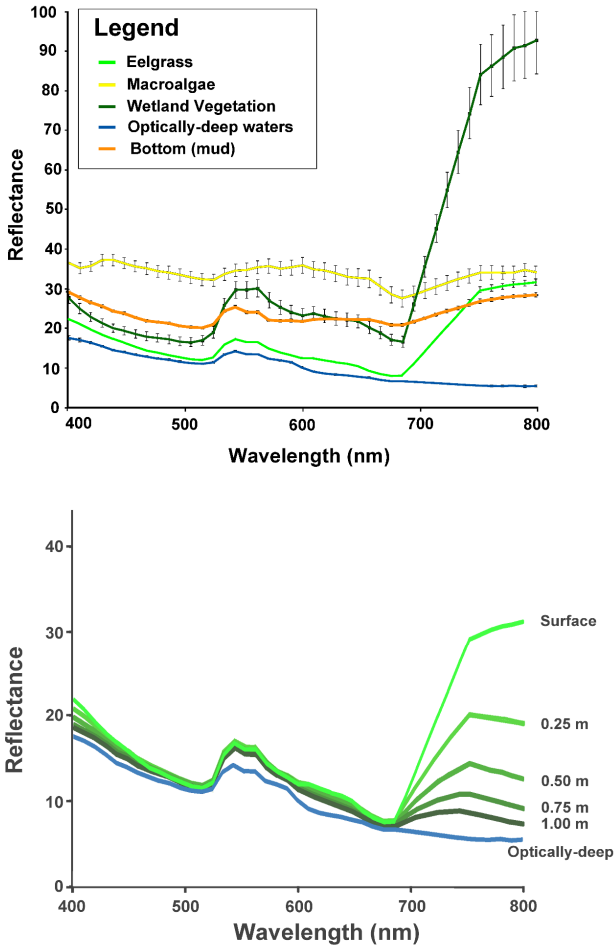

Figure 3. Eelgrass spectra: (top) Spectral signatures with one-standard deviation error bars of the five environmental features used in the HSI eelgrass/macroalgae discrimination procedure. The spectra for the eelgrass, macroalgae, wetland vegetation, and bottom were all taken from above water sites. (Bottom) Spectral signatures of eelgrass exposed and submersed at 0.1, 0.2, 0.3, 0.4, and 0.5 m.

the chlorophyll concentrations measured in Great Bay (134 physical water samples) that were relatively high with a median of 3.4 µg/L and a maximum value of 24.7 µg/L (Trowbridge, 2009). Light scattering from the water will also produce a chlorophyll signature that can confuse the classification algorithms (Volton *et al.*, 1998). Furthermore, exposed bottom, eelgrass, and macroalgae were the only bottom features present both above (exposed land) and below (submersed areas) the water level, whereas wetland vegetation was only present above the water level. Therefore, two separate classification procedures were developed for eelgrass/macroalgae separation of exposed land and submersed areas. The spectral characteristic of the macroalgal signature seemed to be dominated by green macroalgae that occurred around 560 nm (Thorhaug,

Richardson, and Berlyn, 2007), but do not have such a dominant return in the infrared that was characteristic of eelgrass (Alberotanza, Cavalli, and Zandonella, 2006; Thorhaug, Richardson, and Berlyn, 2007; Wezermak, Turner, and Lyzenga, 1976). The lack of a strong return in the infrared can be misinterpreted by some classifiers as eelgrass in deeper waters.

Exposed Land Classification

The exposed land classification procedure included three main steps. First, the vegetation was separated from all non-vegetated areas using the normalized difference vegetation index (NDVI):

$$NDVI_{veg\_isolation} = \frac{R_{rs}(717) - R_{rs}(670)}{R_{rs}(717) + R_{rs}(670)} \quad (2)$$

where, R_{rs} was the remote sensing reflectance and the channel values are in nm.

The specific channels in Equation 2 were chosen based on the spectral characteristics of chlorophyll pigment because of the sharp elevation in reflectance values from 660 nm to 690 nm that peaks around 710 nm to 730 nm, depending on the vegetation (Alberotanza, Cavalli, and Zandonella, 2006; Gitelson, 1992; Haxo and Blinks, 1950; Rundquist *et al.*, 1996; Thorhaug, Richardson, and Berlyn, 2007; Zimmerman, 2003).

The second step was a separation of macroalgae, eelgrass, and wetland vegetation. The spectral characteristics of all three signatures differed in slope along the IR wavelength range between 717 nm and 755 nm (Figure 4). The algorithm used to separate vegetational classes was a Spectral Angle Mapper (SAM) algorithm, also known as the Pearson compliant centered correlation dot product (Cohen, 1988):

$$\alpha = \cos^{-1}\left(\frac{\overrightarrow{U_S} \cdot \overrightarrow{V_R}}{\|\overrightarrow{U_S}\| \cdot \|\overrightarrow{V_R}\|}\right) \quad (3)$$

where, U_S is the sample vector from the imagery compared to a reference signature vector of a given vegetation class V_R. Both vectors contain the reflectance values of the channels between 717 nm and 755 nm. The SAM angle, α, is the numerical resemblance between the sample vector to one of the vegetation spectral signatures. By using the SAM algorithm for separation between the vegetational classes, compared to the commonly used slope measurements of the spectral signatures (*e.g.*, Penuelas *et al.*, 1993; Thorhaug, Richardson, and Berlyn, 2007), data can be processed directly from the HSI and the SAM algorithm's results are less dependent on the spectral resolution of channels.

Underwater Classification

Since optical characteristics of the water limit light transmission to the visible range (with a strong attenuation in the red region, 600 nm to 700 nm), the optically-deep areas were removed to prevent their false classification as vegetation. Channels crossing eelgrass beds were masked using a band ratio. The red/green bands were selected as more appropriate for an estuarine environment based on work by Dierssen *et al.* (2003):

$$\frac{Ln(R_{rs}(547))}{Ln(R_{rs}(630))} \quad (4)$$

In addition, the NDVI algorithm separating vegetated areas from non-vegetated was modified using the 547-nm channel from the green peak in the chlorophyll spectral response with the 630-nm red channel as an absorption low:

$$NDVI_{uderwater} = \frac{R_{rs}(630) - R_{rs}(547)}{R_{rs}(630) + R_{rs}(547)} \quad (5)$$

Since wetland vegetation was not present underwater, the modified NDVI algorithm was sufficient to separate eelgrass and the macroalgae using the green peak of the chlorophyll spectra.

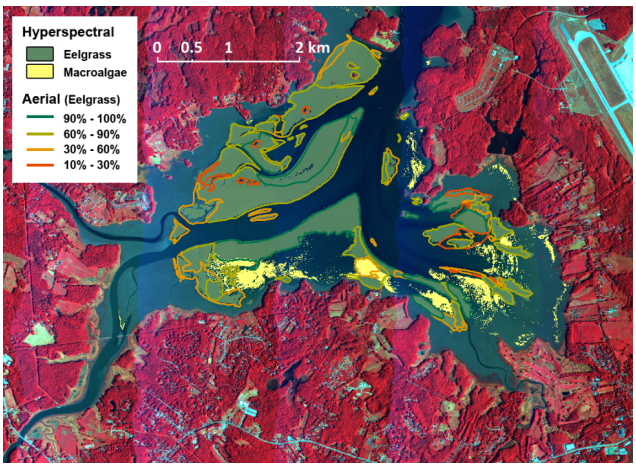

Figure 4. Discrimination procedure results (eelgrass and macroalgae distribution) overlaid on the hyperspectral false color image mosaic (R: 814 nm, G: 670 nm B: 527 nm channels). Eelgrass coverage polygons from the aerial imagery interpretation (Short, 2009) are overlaid on the procedure results.

RESULTS

Spectral discrimination was achieved for eelgrass and macroalgal species in Great Bay (Figure 4). The performance of the decision tree used in the procedure was evaluated based on independent water clarity calculations (Morrison *et al.*, 2008) and manual interpretation supported by field campaigns (Short, 2009). Aerial imagery analysis (Short, 2009) was used as a reference to evaluate the eelgrass detection results of the HSI procedure. Overall, eelgrass classification results using the HSI procedure were 87% true detection (4.38 km^2 out of 5.04 km^2) with 0.27 km^2 of false detection. The accuracy of detection was reduced over sparse eelgrass beds, decreasing from 97% over dense beds (>90% coverage) to 33% over sparse beds (10% to 30% coverage; Table 1). The decrease in detection may be due to the chlorophyll-*a* concentration in waters that can confound this classification. The amount of eelgrass in 2007 using either

Table 1. *Performance evaluation of the discrimination procedure results (HSI) compared to manual interpretation supported by field campaigns (areal) as a function of vegetation density.*

Density	Areal (km^2)	HSI (km^2)	Detection (%)
90%–100%	1.58	1.53	97
60%–90%	2.50	2.33	93
30%–60%	0.73	0.48	66
10%–30%	0.23	0.08	33

HSI or aerial imagery is in contrast to the maximum extent of eelgrass in Great Bay in 1996: 9.80 km^2 (Figure 2).

The procedure detected dense macroalgae in Great Bay in high density areas. In intermixed areas of eelgrass and macroalgae, the procedure identified the areas as eelgrass. A total macroalgal area of 0.84 km^2 was identified. However, there was no ground truthing to validate the results and provide a quantitative estimate. Based on a visual inspection (Short, 2009), it seems that the mapping of high density macroalgae was successful. The locations of most macroalgal beds using the HSI procedure were in the south-central part of Great Bay, predominantly in areas where eelgrass existed in 1996 (Figure 4). Therefore, macroalgal mats have now replaced nearly 9% of the area formerly occupied by eelgrass in Great Bay. Water samples from Great Bay suggest that nitrogen enrichment and water clarity may have affected the eelgrass and caused the proliferation of macroalgae (Trowbridge, 2009; PREP, 2009). It has been reported that total nitrogen concentration of 0.40 mg N/L appears to be a threshold for proliferation of macroalgae species; in Great Bay, the median nitrogen concentration is 0.42 mg N/L. Water clarity is related to total suspended matter, some of which contains chlorophyll. As mentioned in the previous section, chlorophyll concentration measurements in Great Bay were relatively high with a median of 3.4 µg/L and a maximum value of 24.7 µg/L.

DISCUSSION

The procedure developed in this study provides a foundation for future work using hyperspectral imagery. These results demonstrate the ability to provide a benthic classification that differentiates between eelgrass and macroalgae**,** which can improve estuarine monitoring and management. The study showed proliferous growth of green and red nuisance macroalgae in eelgrass habitats (Short, 2009) and confirms NH DES recommendations that photosynthetically available radiation (*i.e.*, integration over the 400 to 700 nm range) and diffuse attenuation should be less than or equal to 0.75 m^{-1} depth (Trowbridge, 2009). The decision was supported by previous studies that indicate a relationship between increased nitrogen loading, light interception by algal producers, and seagrass decline (Burkholder, Tomasko, and Touchette, 2007; Moore and Wetzel, 2000; Neckles *et al*., 1994; Short, Burdick, and Kaldy, 1995; Taylor *et al*., 1995; Twilley *et al*., 1985; Valiela *et al*., 1992, 1997). The detailed results of this study are publically available through New Hampshire's Statewide GIS Clearinghouse, NH GRANIT (http://www.granit.unh.edu/).

The biggest challenge in the procedure was the threshold determination of the optically deep areas (Equation 6) that required a few iterations to determine the deeper areas close to the channels crossing the eelgrass beds. It seems that the dark colors of the vegetation and the water attenuation resulted in under-evaluating the deeper boundaries of eelgrass beds. In the case of Great Bay, the only vegetation close to the channels was eelgrass. Accordingly, a bathymetry DEM dataset collected using lidar or acoustic sensors should be used to calculate the diffuse attenuation coefficient and the extinction depth more accurately than bathymetry generated from the optical imagery. Otherwise, the bathymetry and the bottom classification depend heavily on the water quality and may generate erroneous results. In addition, high concentrations of chlorophyll in the water column (*e.g.*, phytoplankton) may limit bottom detection of SAV. As a result, the procedure is limited to general groups of eelgrass and macroalgae and in the ability to detect successfully eelgrass beds at a density lower than 60%. Unfortunately, eelgrass beds are reduced in winter and early fall when the chlorophyll concentrations are lowest.

CONCLUSIONS

A proof-of-concept procedure was developed for macroalgal and eelgrass mapping based on AISA hyperspectral imagery from a 2007 survey. The procedure is a simplified semi-empirical approach using different classification algorithms for exposed and submersed vegetation. Because the optical characteristics of water limit the light transmission to the visible range, bands in the visible and IR ranges were used for mapping vegetation above the water level and only those in the visible range were used to map submerged vegetation. The classification procedure performed well for high density (>60%) vegetation features (namely, eelgrass). However, it seems that high chlorophyll concentrations in the water column and on the bottom cause background noise that reduces the performance of the classification procedure to map low density vegetation features. The results of the study were used to support the NH DES recommendations for estuarine nutrient criteria.

ACKNOWLEDGMENTS

The project was funded in part by a grant from the Piscataqua Region Estuaries Partnership (PREP) as authorized by the U.S. Environmental Protection Agency's National Estuary Program and UNH/NOAA Joint Hydrographic Center grant NA05NOS4001153. The hyperspectral imagery was collected by SpecTIR. Published as Scientific Contribution #523 from the Jackson Estuarine Laboratory. Also, the authors would like to thank the anonymous reviewers for their comments that have improved the manuscript.

LITERATURE CITED

Ackleson, S.G. and Klemas, V., 1987. Remote sensing of submerged aquatic vegetation in lower Chesapeake Bay: a comparison of Landsat MSS to TM imagery. *Remote Sensing of Environment*, 22, 235–248.

Alberotanza, LR.M.; Cavalli, S.P., and Zandonella, A., 2006. Classification of submerged aquatic vegetation of the Venice lagoon using MIVIS airborne data. *Annals of Geophysics*, 49(1), 271–276.

Beem, N.T. and Short F.T., 2009. Subtidal eelgrass declines in the Great Bay Estuary, New Hampshire and Maine, USA. *Estuaries and Coasts*, 32, 202–205.

Beiwirth, P.N.; Lee, T.J., and Burne, R.V., 1993. Shallow seafloor reflectance and water depth derived by unmixing multispectral imagery. *Photogrammetric Engineering and Remote Sensing*, 59, 331–338.

Brando, V.E. and Dekker, A.G., 2003. Satellite hyperspectral remote sensing for estimating coastal water quality. *IEEE Transactions on Geoscience and Remote Sensing*, 41(6), 1378–1387.

Bricker, S.B.; Longstaff, B.; Dennison, W.; Jones, A.; Boicourt, K.; Wicks, C., and Woerner, J., 2008. Effects of nutrient enrichment in the nation's estuaries: A decade of change. *Harmful Algae*, 8, 21–32.

Burkholder, J.A.; Tomasko, D.A., and Touchette, B.W., 2007. Seagrasses and eutrophication. *Journal of Experimental Marine Biology and Ecology*, 350, 46–72.

Casal, G.; Sánchez-Carnero, N.; Domínguez-Gomez, J.A.; Kutser, T., and Freire, J., 2012. Assessment of AHS (Airborne Hyperspectral Scanner) sensor to map macroalgal communities on the Ria de Vigo and Ria de Aldan coast (NW Spain). *Marine Biology*, 159, 1997–2013.

Chock, J.S., and Mathieson, A.C., 1983. Variations of New England estuarine seaweed biomass. *Botanica Marina*, 26, 87–97.

Cohen, J., 1988. *Statistical Power Analysis for the Behavioral Sciences (2nd ed.).* Hillsdale, New Jersey: Erlbaum, 590p.

Costa, J.E.; Howes, B.L.; Giblin, A.E., and Valiela I., 1992. Monitoring nitrogen and indicators of nitrogen loading to support management action in Buzzards Bay, *In:* McKenzie, D.H.; Hyatt, D.E., and V.J. McDonald (eds.), *Ecological Indicators*. New York: Elsevier Applied Science, pp. 499–531.

Dekker A.G.; Zamurović-Nenad, Z.; Hoogenboom, H.J., and Peterset, S.W.M., 1996. Remote Sensingecological water quality modeling and *in situ* measurements: A case study in shallow lakes. *Hydrological Sciences Journal*, 41(1), 531–547.

Dekker, A.G.; Brando, V.E.; Anstee, J.M.; Pinnel, N.; Kutser, T.; Hoogenboom, E.; Peters, S.; Pastercamp, R.; Vos, R.; Olbert, C., and Malthus, T.J.M., 2002. Imaging spectrometry of water. *In:* van-der Meer, F. and De. Jong, S.M. (eds.), *Imaging Spectrometry: Basic Principles and Prospective Applications*. Netherlands: Springer, pp. 307–359.

Dekker, A.G.; Brando, V.E.; Anstee, J.M.; Fyfe, S.; Malthus, T.J.M., and Karpouzli, E., 2006. Remote sensing of seagrass ecosystems: use of spaceborne and airborne sensors. *In:* Larkum, A.W.D.; Orth, R.J., and C.M. Duarte (eds.), *Seagrasses: Biology, Ecology and Conservation*. Netherlands: Springer, pp. 347–359.

Dierssen, H.M.; Zimmerman, R.C.; Leathers, R.A.; Downes, V., and Davis, C.O., 2003. Ocean color remote sensing of seagrass and bathymetry in the Bahamas Banks by high-resolution airborne imagery. *Limnology and Oceanography*, 48, 444–455.

Drake, L.A.; Dobbs, F.C., and Zimmerman, R.C., 2003. Effects of epiphyte load on optical properties and photosynthetic potential of the seagrasses *Thalassia testudinum* Banks ex König and *Zostera marina*. *Limnology and Oceanography*, 48(1, part 2), 456–463.

Dring, M.J., 1991. *The Biology of Marine Plants*. London: Cambridge University Press, 208p.

Duarte, C.M., 1991. Seagrass depth limits. *Aquatic Botany*, 40(4), 363–377.

Ferguson, R.L. and Korfmacher, K., 1997. Remote sensing and GIS analysis of seagrass meadows in North Carolina, USA. *Aquatic Botany*, 58, 241–258.

Fyfe, S.K., 2003. Spatial and temporal variation in spectral reflectance: Are seagrass species spectrally distinct. *Limnology and Oceanography*, 48(1, part 2), 464–479.

Gitelson, A., 1992. The peak near 700 nm on reflectance spectra of algae and water: relationships of its magnitude and position with chlorophyll concentration. *International Journal of Remote Sensing*, 13, 3367–3373.

Hardwick-Witman, M.N. and Mathieson, A.C., 1983. Intertidal macroalgae and macroinvertebrates: Seasonal and spatial abundance patterns along an estuarine gradient. *Estuarine, Coastal and Shelf Science*, 16, 113–129.

Hauxwell, J.; Cabrien, J., and Valiela, I., 2003. Eelgrass *Zostera marina* loss in temperate estuaries: relationship to land-derived nitrogen loads and effect of light limitation imposed by algae. *Marine Ecology Progress Series*, 247, 59–73.

Haxo, F.T. and Blinks, L.R., 1950. Photosynthetic action spectra of marine algae. *The Journal of General Physiology*, 33, 389–422.

Jackson, C.F., 1944. *A biological survey of Great Bay*. Durham, New Hampshire: New Hampshire by the Marine Fisheries *Commission. State Planning Development Commission Report*, 61p.

Jakobsson, M.; Armstrong, A.A.; Calder, B.; Huff, L.; Mayer, L., and Ward, L., 2005. On the use of historical bathymetric data to determine changes in bathymetry. *International Hydrographic Review*, 6(3), 35–41.

Jerlov, N.G., 1976. *Marine optics*. Amsterdam: Elsevier, 230p.

Josselyn, M., 1978. The contribution of marine macrophytes to the detrital pool of the Great Bay Estuary System, NH. Durham, New Hampshire: University of New Hampshire, Ph.D. dissertation, 141p.

Josselyn, M. and Mathieson, A.C., 1980. Seasonal influx and decomposition of autochthonous macrophyte litter in a north temperate estuary. *Hydrobiologia*, 71, 197–208.

Karpouzli, E.; Malthus, T.J., and Place, C.J., 2004. Hyperspectral discrimination of coral reef benthic communities in the western Caribbean. *Coral Reefs*, 23(1), 141–151.

Kirk, J.T.O., 1994. *Light and Photosynthesis in Aquatic Ecosystems* (2nd Edition). New York: Cambridge University Press, 509p.

Kirkpatrick, G.J.; Orrico, C.; Moline, M.A.; Oliver, M., and Schofield, O.M., 2003. Hyperspectral absorption measurements of colored dissolved organic material in aquatic systems. *Applied Optics*, 42(33), 6564–6568.

Kutser, T.; Miller, I., and Jupp, D.L.B., 2006. Mapping coral reef benthic substrates using hyperspectral space-borne images and spectral libraries. *Estuarine, Coastal and Shelf Science*, 70, 449–460.

Larsen, F.; Phinney, D.A.; Rubi, F., and Justice, D., 2009. Classification of boreal macrotidal littoral zone habitats in the

Gulf of Maine: comparison of IKONOS and CASI multispectral imagery. *Geocarto International*, 24(6), 457–472.

Lippmann, T.C. and Smith, G.M., 2009. Shallow surveying in hazardous waters. *Proceedings in U.S. Hydrographic Conference* (Norfolk, Virginia).

Lyzenga D.R.; Malinas, N.P., and Tanis, F.J., 2006. Multispectral bathymetry using a simple physically based algorithm. *IEEE Transaction on Geosciences and Remote Sensing*, 44, 2251–2259.

Mathieson, A.C. and Hehre. E.J., 1986. A synopsis of New Hampshire seaweeds. *Rhodora*, 88, 1–139.

Mathieson, A.C. and Penniman, C.A., 1986. Species composition and seasonality of New England seaweeds along an open coastal-estuarine gradient. *Botanica Marina*, 29, 161–176.

Mathieson, A.C. and Penniman, C.A., 1991. Floristic patterns and numerical classification of New England estuarine and open coastal seaweed populations. *Nova Hedwigia*, 52, 453–485.

McGlathery, K.J.; Sundback, K., and Anderson, I.C., 2007. Eutrophication in shallow coastal bays and lagoons: The role of plants in the coastal filter. *Marine Ecology Progress Series*, 348, 1–18.

Macleod, R.; Congalton, R., and Short, F., 1995. Using quantitative accuracy assessment techniques to compare various change detection algorithms for monitoring eelgrass distributions in Great Bay, NH generated from Landsat TM data. *Proceedings of the Sixty-First Annual Meeting of the American Society of Photogrammetry and Remote Sensing* (Charlotte, North Carolina), Volume 3, pp. 876–885.

McKenzie, L.J.; Finkbeiner, M.A., and Kirkman, H., 2001. Methods for mapping seagrass distribution. *In:* Short, F.T. and Coles, R.G. (eds.), *Global Seagrass Research Methods*. Amsterdam, The Netherlands: Elsevier, pp. 101–121.

Milne L.J. and Milne, M.J., 1951. The eelgrass catastrophe. *Scientific American*, 184, 52–55

Moore, K.A. and Wetzel, R.L., 2000. Seasonal variations in eelgrass (*Zostera marina L.*) responses to nutrient enrichment and reduced light availability in experimental systems. *Journal of Experimental Marine Biology and Ecology*, 244, 1–28.

Morrison, J.R.; Gregory, T.K.; Pe'eri, S.; McDowell, W., and Trowbridge, P., 2008. *Using Moored Arrays and Hyperspectral Aerial Imagery to Develop Nutrient Criteria for New Hampshire's Estuaries*. Durham, New Hampshire: A Final Report to the New Hampshire Estuaries Project from the University of New Hampshire, 65p.

Mumby, P.J.; Green, E.P.; Edwards, A.J., and Clark, C.D., 1997. Coral reef habitat mapping: How much detail can remote sensing provide? *Marine Biology*, 130, 193–202.

National Oceanic and Atmospheric Administration (NOAA), 2013. *Portsmouth to Dover and Exeter (12th edition)*, *Chart 13285*. Silver Spring, Maryland: NOAA, scale: 1:20,000, 1 sheet.

Neckles, H.A.; Koepfler, E.T.; Haas, L.W.; Wetzel, R.L., and Orth, R.J., 1994. Dynamics of epiphytic photoautotrophs and heterotrophs in *Zostera marina* L. (eelgrass) microcosms: Responses to nutrient enrichment and grazing. *Estuaries*, 17, 597–605.

Ochieng, C.A.; Short, F.T., and Walker D.I., 2010. Effect of light on plant parameters and photosynthetic characteristics of eelgrass (*Zostera marina* L.): a mesocosm experiment. *Journal of Experimental Marine Biology and Ecology*, 382, 117–124.

Odell, J.; Eberhardt, A.; Burdick, D., and Ingraham, P., 2006. *Great Bay Estuary Restoration Compendium*. Durham, New Hampshire: New Hampshire Estuaries Program (NHEP) Report, 65p.

Olesen, B. and Sand-Jensen, K., 1993. Seasonal acclimatization of eelgrass Zostera Marina growth to light. *Marine Ecology Program Series*, 94, 91–99.

Pasqualini, V.; Pergent-Martini, C.; Pergent, G.; Agreil, M.; Skoufas, G.; Sourbes, L., and Tsirika, A., 2005. Use of SPOT 5 for mapping seagrasses: an application to Posidonia oceanica. *Remote Sensing of Environment*, 94(1), 39–45.

Pe'eri, S.; Parrish, C.E.; Azuike, C.; Alexander, L., and Armstrong, A., 2014. Remote sensing as a reconnaissance tool for assessing nautical chart adequacy and completeness. *Marine Geodesy*, 37(3), 293–314.

Peneva, E.; Griffith, J.A., and Carter, G.A., 2008. Seagrass mapping in the northern Gulf of Mexico using airborne hyperspectral imagery: a comparison of classification methods. *Journal of Coastal Research*, 24(4), 850–856.

Penuelas, J.; Field, C.; Griffin, K., and Gamon, J., 1993. Assessing community type, plant biomass, pigment composition, and photosynthetic efficiency of aquatic vegetation from spectral reflectance. *Remote Sensing of Environment*, 46, 110–118.

Philpot, W.D., 1989. Bathymetric mapping with passive multispectral imagery. *Applied Optics,* 28(8), 1569–1578

Philpot, W.D.; Davis, C.O.; Bissett, W.P.; Mobley, C.D.; Kohler, D.D.R.; Lee, Z.; Bowles, J.; Steward, R.G.; Agrawal, Y.; Trowbridge, J.; Gould R.W., and Arnone, R.A., 2004. Bottom characterization from hyperspectral image data. *Oceanography*, 17(2), 76–85.

Phinn, S.; Roelfsema, C.; Dekker, A.; Brando, V., and Anstee, J., 2008. Mapping seagrass species, cover and biomass in shallow waters: An assessment of satellite multi-spectral and airborne hyper-spectral imaging systems in Moreton Bay (Australia). *Remote Sensing of Environment*, 112, 3413–3425.

Piscataqua Region Estuaries Partnership (PREP), 2009. *State of the Estuaries*. Durham, New Hampshire: PREP Report, 32p.

Rundquist, D.C.; Han, L.; Schalles, J.F., and Peake, J.S., 1996. Remote measurement of algal chlorophyll in surface waters: the case for the first derivative of reflectance near 690 nm. *Photogrametric Engineering and Remote Sensing*, 62, 195–200.

Short, F.T., 1992. *The ecology of Great Bay Estuary, New Hampshire and Maine: An Estuarine Profile and Bibliography*. Durham, New Hampshire: NOAA Coastal Ocean Program Publication, 222p.

Short, F.T., 2009. *Eelgrass Distribution in the Great Bay Estuary for 2008*. Durham, New Hampshire: University of New Hampshire report to the Piscataqua Region Estuaries Partnership, 7p.

Short, F.T., 2012. *Eelgrass Distribution in the Great Bay Estuary for 2011*. Durham, New Hampshire: University of New Hampshire report to the Piscataqua Region Estuaries Partnership, 7p.

Short, F.T. and Burdick, D.M., 1996. Quantifying eelgrass habitat loss in relation to housing development and nitrogen loading in Waquoit Bay, Massachusetts. *Estuaries*, 19, 730–739.

Short, F.T.; Burdick, D.M., and Kaldy, J.E., 1995. Mesocosm experiments quantify the effects of eutrophication on eelgrass, *Zostera marina*. *Limnology and Oceanography*, 40, 740–749.

Short, F.T.; Mathieson, A.C., and Nelson, J.I., 1986. Recurrence of the eelgrass wasting disease at the border of New Hampshire and Maine, USA. *Marine Ecology Progress Series*, 29, 89–92.

Short, F.T. and Short, C.A., 1984. The seagrass filter: purification of coastal water. *In:* Kennedy, V.S. (ed.), *The Estuary as a Filter,* Orlando, Florida: Academic Press, pp. 395–413.

Short, F.T. and Trowbridge, P., 2003. *UNH eelgrass (Zostera marina) monitoring program*. Concord, New Hampshire: Quality assurance project plan, 13p.

Short, F.T. and Wyllie-Echeverria, S., 1996. Natural and human-induced disturbance of seagrasses. *Environmental Conservation*, 23, 17–27.

Taylor, D.I.; Nixon, S.W.; Granger, S.L.; Buckley, B.A.; McMahon, J.P., and Lin, H.-J., 1995. Responses of coastal lagoon plant communities to different forms of nutrient enrichment a mesocosm experiment. *Aquatic Botany*, 52, 19–34.

Thorhaug, A.; Richardson, A.D., and Berlyn, G.P., 2007. Spectral reflectance of the seagrasses: *Thalassia testudinum*, *Halodulewrightii*, *Syringodium filiforme* and five marine algae. *International Journal of Remote Sensing*, 28(7), 1487–1501.

Trowbridge, P., 2009. *Numeric Nutrient Criteria for the Great Bay Estuary*. Concord, New Hampshire: New Hampshire Department of Environmental Services Technical Report, 92p.

Twilley, R.R.; Kemp, W.M.; Staver, K.W.; Stevenson, J.C., and Boynton, W.R., 1985. Nutrient enrichment of estuarine submersed vascular plant communities. 1. Algal growth and effects on production of plants and associated communities. *Marine Ecology Progress Series*, 23, 179–191.

Vahtmäe, E.; Kutser, T.; Martin, G., and Kotta, J., 2006. Feasibility of hyperspectral remote sensing for mapping macroalgal cover in turbid coastal waters- a Baltic Sea case study. *Remote Sensing of Environment*, 101, 342–351.

Valiela, I.; Foreman, K.; LaMontagne, M.; Hersh, D.; Costa J., and Peckol, P., 1992. Couplings of watersheds and coastal waters: sources and consequences of nutrient enrichment in Waquoit Bay, Massachusetts. *Estuaries*, 15, 443–457.

Valiela, I.; McClelland, J.; Hauxwell, J.; Behr, P.J.; Hersh, D., and Foreman, K., 1997. Macroalgal blooms in shallow estuaries: control and ecophysiological and ecosystem consequences. *Limnology and Oceanography*, 42, 1105–1118.

Volton, H.; De Haan, J.F.; Hovenier, J.W.; Schuers, R.; Vassen, W.; Dekker, A.G.; Hoogenboon, H.J.; Charelton, F., and Wouts, R., 1998. Laboratory measurements of angular distribution of light scattered by phytoplankton and silt. *Limnology and Oceanography*, 43, 1180–1197.

Wezernak, C.T.; Turner R.E., and Lyzenga, D.R., 1976. *Spectral reflectance and radiance characteristics of water pollutants*, NASA CR-2665, pp. 110–111.

Yu, Q.; Tian, Y.Q.; Chen, R.F.; Liu, A.; Gardner, G.B., and Zhu, W., 2010. Functional linear analysis of in situ hyperspectral data for assessing CDOM in rivers. *Photogrammetric Engineering and Remote Sensing*, 76(10), 1147–1158.

Zibordi, G.; Parmiggiani, F., and Alberotanza, L., 1990. Application of aircraft multispectral scanner data to algae mapping over the Venice lagoon, *Remote Sensing of Environment*, 34, 49–54.

Zimmerman, R.C., 2003. A biooptical model of irradiance distribution and photosynthesis in seagrass canopies. *Limnology and Oceanography*, 48, 568–585.

Zimmerman, R.C., 2006. Light and photosynthesis in seagrass meadows. *In:* Larkum, A.W.D.; Orth, R.J., and C.M. Duarte (eds.), *Seagrasses: biology, ecology and conservation*. Netherlands: Springer, pp. 303–321.